Approaching Ultimate SNR with Finite Coil Arrays

F. Wiesinger[1], N. De Zanche[1], K. P. Pruessmann[1]

[1]Institute for Biomedical Engineering, University Zurich and ETH, Zurich, Switzerland

Introduction:

In the late 1980s, Roemer et al. revolutionized signal reception in MRI by introducing phased-array coils (1). Array reception permits an increase in the SNR yield by covering the imaged region with multiple coils having individual localized reception characteristics. In parallel imaging (PI) the parallel nature of array reception is utilized to provide supplementary spatial encoding. Recently the ultimate intrinsic SNR limitations of PI have been identified and explored in detail (2,3). Most importantly it was found that: (I) the amount of feasible reduction in PI is inherently limited and (II) PI performance significantly improves from onsetting far-field wave behavior at high field strengths (B_0) and/or large object sizes. The fundamental benefits of far-field effects have also been demonstrated experimentally (4). However it is not clear yet to which extent the ultimate SNR limit can be approached with finite coil setups. In this work we calculate the PI performance of model arrays consisting of a finite number of discrete, circular current distributions and compare it with the theoretical SNR limit established in Ref. (3).

Theory and Methods:

The model setup consists of a conductive, dielectric, spherical object assumed to be evenly surrounded by concentrically-arranged, circular coils of finite resistance. An even distribution of N identical RF coil elements over the whole sphere was achieved via iterative, numerical optimization. The coil radius was chosen so that neighboring elements touch but do not overlap (cf. Fig. 1). The advantages of this specific arrangement are: (I) it allows to semi-analytically express the full-wave RF electrodynamic fields (5) and (II) the choice of a spherical object permits direct comparisons with the ultimate SNR (SNR_U) performance determined in Ref. (3).

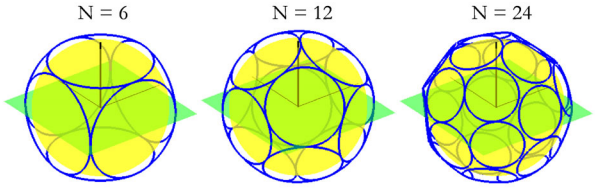

FIGURE 1: Coil arrangements for various numbers of coil elements (N). The coil packing was optimized numerically. For certain N (4, 6, 8, 12, 20) the optimization yields the analogue of a platonic solid.

For a realistic SNR calculation both sample losses and coil conductor losses were taken into account. Based on the coil sensitivity matrix (S) and the receiver noise matrix (Ψ) the electrodynamic dependencies of SNR were investigated according to (3,6):

$$\mathrm{SNR}\left(R, N, B_0, \ldots\right) \propto B_0^2 \Big/ \sqrt{(S^H \psi^{-1} S)^{-1}}\,. \qquad [1]$$

The dimensions of the spherical object were chosen to be an approximate model of the human head with a diameter of 0.2 m, and dielectric properties mimicking those of average in-vivo brain (7). For the modeling of conductor losses, the resistance of a typical unloaded surface coil was determined experimentally via a Q-factor measurement. The resistance was subsequently adapted to the required coil diameters and resonance frequencies utilizing fundamental physical scaling relations (8). All SNR evaluations were performed for a central, transverse imaging plane. The circular coils were concentrically distributed around the object on a spherical shell of 0.22 m in diameter (cf. Fig. 1). To assess PI performance systematically Eq. [1] was separately analyzed in terms of (I) the SNR obtained for full Fourier encoding; i.e. with reduction factor R≡1 and (II) the geometry factor (g), according to (6):

$$\mathrm{SNR}(R, N, B_0, \ldots) = \mathrm{SNR}(R \equiv 1) \big/ \sqrt{R}\, g\,. \qquad [2]$$

Results and Discussion:

Figure 2 shows the convergence of SNR towards its ultimate value in terms of SNR / SNR_U for R ≡ 1 as a function of N. Three different field strengths B_0 = 1.5, 4.5, 7.5 T and three different amounts of eccentricity of the reconstructed pixel r_0 = 0 m (left), 0.05 m (middle), 0.09 m (right) are considered. For the case when only sample losses were taken into account (i.e., no marker), central ultimate SNR (i.e. r_0 = 0) can be readily approached with a finite coil arrangement. However, when coil losses are also taken into account (i.e., '*' marker) the SNR yield becomes significantly decreased. This is especially the case at low B_0 when the noise is less sample dominated. Furthermore, the convergence of SNR to its theoretical maximum is also reduced for locations with high values of r_0 and/or B_0. In these cases more (and hence smaller) coils would be required, either to be specifically sensitive at locations close to the surface, or in order to efficiently take advantage of the field focusing capabilities at high B_0.

Figure 3 illustrates the convergence of g(R) towards the ultimate g-factor (g_U) for r_0 = 0 m as a function of N. Several field strengths B_0 = 1.5, 4.5, 7.5 and 10.5 T and reduction factors in the range of 1 and 6 are considered. Again with increasing N the g factors converge towards their corresponding ultimate values. However, the speed of the convergence reduces with increasing R. This reflects the central pixel's entanglement with peripheral pixels for R > 2.

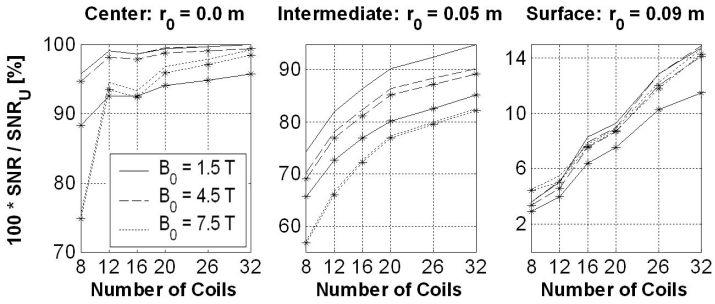

FIGURE 2: SNR normalized to the theoretical ultimate SNR versus number of coil elements for variable r_0 and B_0. r_0 denotes the distance of the reconstructed pixel from the center of the sphere. The marker '*' indicates results obtained taking into account finite coil losses.

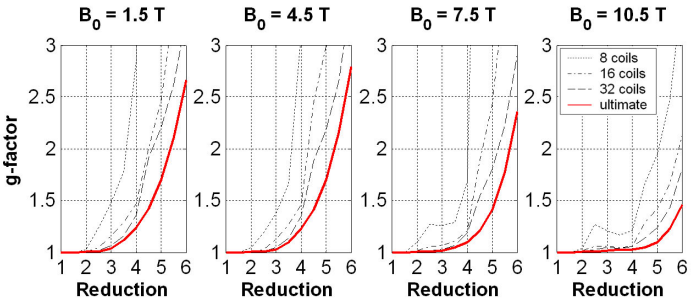

FIGURE 3: Evaluation of g-factor performance versus the reduction factor (R) for different numbers of coil elements and different B_0. Here only central reconstruction is considered (r_0=0). For comparison the ultimate g-factor (red line) is also shown.

It has been suggested that coil losses will impose a practical limit on the number of coils. Ultimately it is expected that SNR will begin to decrease beyond some critical N, even more so when, preamplifier noise is taken into account. In general this specific value of N will depend on the conductivity and the size of the object, B_0 and technical RF parameters such as the coil conductor resistance and the noise figure of the preamplifier.

Note that for different N's different densities of surface coverage is obtained; i.e., N = 12 results in a comparably, highly efficient pentagon-dodecahedral coil packing with 5 closest neighbors for each coil. This may explain the slight irregularities in the otherwise smooth convergence of the SNR and g in Figs. 2 and 3.

Furthermore, preliminary results do indicate that coil overlap becomes less critical for PI unfolding using large coil arrays (9). This possibly has to do with the encoding redundancy provided by a large number of closely spaced coils, where each reconstruction location is surrounded by multiple closely neighboring elements. However, the general question of which circular coil arrangement is optimal (i.e. regarding number of elements, packing, overlap) will require further investigation.

References:

[1] Roemer PB, et al (1990) MRM 16:192-225.
[2] Ohliger MA, et al (2003) MRM 50(5):1018-1030.
[3] Wiesinger F, et al (2004) MRM 52:376-390.
[4] Wiesinger F, et al (2004) MRM 52:953-964.
[5] Keltner JR, et al (1991) MRM 22: 467-480.
[6] Pruessmann KP, et al (1999) MRM 42:952-962.
[7] Gabriel S, et al (1996) PhysMedBiol 41:2271-2293.
[8] Jackson JD, Classical Electrodynamics (1999).
[9] Weiger M, et al (2001) MRM 45:495-503.